

The Expression Level of Inflammation-Related Genes in Patients With Bone Nonunion and the Effect of BMP-2 Infected Mesenchymal Stem Cells Combined With nHA/PA66 on the Inflammation Level of Femoral Bone Nonunion Rats

Yong HUANG¹, Qin ZHANG¹, Qingling JING¹, Xiandeng LI¹, Fanhui DONG²

¹Department of Orthopedic Surgery, Qing Hai University Affiliated Hospital, Xining, Qinghai, China,

²Department of Pain Physiotherapy, People's Hospital of Rizhao, Rizhao, Shandong, China

Received March 5, 2024

Accepted June 27, 2024

Summary

Bone nonunion delays fracture end repair and is associated with inflammation. Although bone nonunion can be effectively repaired in clinical practice, many cases of failure. Studies have confirmed that BMP-2 and nHA/PA66 repaired bone defects successfully. There are few studies on the effects of the combined application of BMP-2 and NHA/PA66 on bone nonunion osteogenesis and inflammation. We aimed to investigate the expression level of inflammation-related genes in patients with bone nonunion and the effect of BMP-2-infected mesenchymal stem cells combined with nHA/PA66 on the level of inflammation in femur nonunion rats. We searched for a gene expression profile related to bone nonunion inflammation (GSE93138) in the GEO public database. Bone marrow mesenchymal stem cells (MSCs) of SD rats were cultured and passed through. We infected the third generation of MSCs with lentivirus carrying BMP-2 and induced the infected MSCs to bone orientation. We detected the expression level of BMP-2 by RT-PCR and the cell viability and alkaline phosphatase (ALP) activity by CCK8 and then analyzed the cell adhesion ability. Finally, the levels of related inflammatory factors, including C-reactive protein (CRP), interleukin-6 (IL-6), tumor necrosis factor- α (TNF- α) and Erythrocyte Sedimentation Rate (ESR), were detected in nonunion rats. Our findings: The patients with nonunion had up-regulated expression of 26 differentially inflammatory genes. These genes are mainly enriched in innate immune response, extracellular region, calcium ion binding, Pantothenate and CoA biosynthesis pathways. The expression level of BMP-2 in the Lenti-BMP-2 group was higher (vs. empty lentivirus vector group: $t=5.699$; vs. uninfected group $t=3.996$). The cell activity of the MSCs + BMP-2 + nHA/PA66 group

increased gradually. After being combined with nHA/PA66, MSCs transfected with BMP-2 spread all over the surface of nHA/PA66 and grew into the material pores. MSCs + BMP-2 + nHA/PA66 cells showed positive ALP staining, and the OD value of ALP was the highest. The levels of CRP, IL-6, TNF- α , and ESR in the MSCs + BMP-2 + nHA/PA66 group were lower than those in the MSCs and MSCs + nHA/PA66 group but higher than those in MSCs + BMP-2 group. The above comparisons were all $P<0.05$. The findings demonstrated that the expression level of inflammation-related genes increased in the patients with bone nonunion. The infection of MSCs by BMP-2 could promote the directed differentiation of MSCs into osteoblasts in the bone marrow of rats, enhance the cell adhesion ability and ALP activity, and reduce inflammation in rats with bone nonunion.

Key words

Inflammation • Bone nonunion • Femoral • BMP-2
• Mesenchymal stem cells • nHA/PA66

Corresponding author

F. Dong, Department of Pain Physiotherapy, People's Hospital of Rizhao, 126 Taian Street, Rizhao 276800, Shandong, China.
E-mail: 17697119395@163.com

Introduction

Bone nonunion means that the fracture cannot heal, and the typical manifestations are persistent pain, deformity and loss of function, and psychosocial disability, with an incidence of 10 % [1]. Bone nonunion delays the repair of the fracture, seriously reducing the

patient's quality of life. Bone nonunion effective repair measures often involve debridement, bone grafting, fixation, etc., but there are still many failure cases.

Many factors, such as nutrition, systemic diseases, fracture type, infection, and surgical quality, can affect fracture healing and cause bone nonunion [2]. Although medical researchers have confirmed that these factors are the causes at the macro level, it is rare to analyze bone nonunion at the molecular level (genes or cytokines such as growth factors, cytokines, chemokines, etc.). Abnormalities in these complex molecules necessary for bone repair can lead to delayed bone healing [3,4]. Previous studies [5] have shown that fractures are accompanied by increased inflammatory factors and slow healing, which seriously affect prognosis. Chronic inflammation inhibits bone formation and promotes bone resorption, in which bone stem cells exhibit defects, resulting in impaired osteogenic differentiation. Inflammatory cytokines such as interleukin-6 (IL-6) and tumor necrosis factor- α (TNF- α) have been proven to regulate fracture healing [6]. In addition, the inflammatory response was accompanied by abnormal changes in CRP and ESR.

Mesenchymal stem cells (MSCs) derived from bone marrow matrix have the potential to differentiate into bone, cartilage, muscle and other tissues [7]. Bone morphogenetic protein 2 (BMP-2) can promote the directed differentiation of MSCs into osteoblasts [8]. Nano-hydroxyapatite/polyamide 66 (nHA/PA66) is a polymeric material composed of hydroxyapatite and polyamide 66. nHA/PA66 is close to bone tissue composition and structure and has good biocompatibility, mechanical properties and bone conductivity [9]. nHA/PA66 has been successfully applied in artificial vertebrae and laminae as bone-filling materials to repair bone defects [10]. There is still a lack of studies on nHA/PA66 in bone nonunion application.

We implanted BMP-2 infected rat MSCs into the femoral fracture of SD rats, then constructed the tissue-engineered bone by combining BMP-2 with nHA/PA66 to study the effect of BMP-2 on bone healing and the level of inflammation in the diseased area.

Materials and Methods

Expression of inflammatory related differential genes in patients with bone nonunion

“Nonunion”, “bone fractures” and “homo sapiens” as keywords, the GEO public database

(<https://www.ncbi.nlm.nih.gov/gds/>) [11] retrieval in patients with bone nonunion of gene expression profile, Peripheral blood bone nonunion chip GSE93138 was obtained, including 8 patients with acute injury fracture nonunion and 4 healthy volunteers, whose platform was GPL6244. The genes associated with inflammation were obtained from the Genecard database, which contains 12365 genes. Use the “GEO2R” of GEO to screen the differentially expressed genes between bone nonunion samples and healthy samples ($|\log FC| > 2$ and $P < 0.05$ after correction as the threshold). We intermixed the screened differentially expressed genes with inflammation-related genes. Finally, we obtained the expression of inflammation-related differentially expressed genes in patients with bone nonunion and enriched the inflammatory differential genes by KEGG and GO.

Experimental rat sources and data, stent materials, reagents, and instruments

30 SPF SD rats (10 for stem cell extraction and 20 for *in vivo* experiment), both male and female, aged 7-8 weeks and weighing 190-225 g, were provided by the Chengdu Dashuo Experimental Animal Co., LTD. Feeding conditions were: Temperature 18-26 °C, relative humidity 40-70 % (the temperature in the feeding box is 1-2 °C higher and humidity 5-10 % higher than the environment). Noise is below 85 decibels, ammonia concentration below 20 ppm; Ventilate 8-12 times/h.

Porous bionic bone scaffold material nHA/PA66 is provided by Guona Technology Co., LTD. DMEM/F12, dexamethasone, sodium betaglycerophosphate, ascorbic acid (Luwei Pharmaceutical Group Limited); Fetal bovine serum (Wuhan Punosai Life Technology Co., LTD.); Pancreatic enzyme cell digestive fluid (containing 0.25 % pancreatic enzyme and 0.02 % EDTA), penicillin, streptomycin, 10 % chlora hydrate (Sichuan Vicchi Biotechnology Co., LTD.); Flow cytometry (Beckman Coulter); Alkaline phosphatase test kit (enzyme labelling method) (Shanghai Coaibo Biological); CO₂ incubator (Shanghai Dute Scientific Instrument Co., LTD.); Inverted Phase contrast microscopy and Photographic System (Olympus); MolecularDevices; Micro CT (Scanco Medical).

Isolation and culture of rat bone marrow MSCs, osteogenesis induction, and BMP-2 infection

MSCs of rat bone marrow were isolated by whole bone marrow adherent culture. Both femurs and tibia were

removed under aseptic conditions, epiphysis was removed at both ends of the long bones, and bone marrow in the medullary cavity was slowly rinsed with stem cell medium and transferred into culture bottles. Primary cells were cultured with DMEM/F12 containing 20 % fetal bovine serum by volume. 3 days later, after the first fluid change, when the cells reached 70 % to 80 % fusion, the cells were digested with trypsin, passed according to the ratio of 1:2, and changed to DMEM/F12 culture medium containing 10 % fetal bovine serum by volume. Bone marrow MSCs were identified by flow cytometry.

We applied the 3rd generation rat bone marrow MSCs for osteogenic induction differentiation. The osteogenic induction solution contained 10 % fetal bovine serum, dexamethasone (100 nmol/l), β -sodium glycerophosphate (10 mmol/l) and ascorbic acid (0.05 mmol/l). We replaced the osteogenic induction solution every two days. We take cells cultured in DMEM/F12 medium containing 10 % fetal bovine serum by volume as controls. Finally, we observed the cell adhesion, growth, proliferation, morphological changes, and morphology of rat bone marrow MSCs in an inverted phase contrast microscope.

The third generation of cultured cells were infected with lentiviral vectors (Lenti-BMP-2 and Lenti-NC, the construction, packaging and purification of lentiviral vectors were entrusted to Yunzhou Biotechnology Co., LTD.) with infection multiple (MOI=25). We divided the cells into Lenti-BMP-2, empty lentiviral vector and uninfected group (all n=10). We amplified the three groups of cells by amplifying HT1080 cells, and then the expression level of BMP-2 was detected by reverse transcription polymerase chain reaction (RT-PCR). The RNA was extracted and tested by an ultraviolet spectrophotometer. OD value (A_{260}/A_{280}) was 1.8~2.0. Synthesize the mRNA with good integrity by gel electrophoresis. Perform the extraction of total RNA and cDNA synthesis according to the kit instructions. Reverse transcription system, reaction conditions, PCR system, and reaction parameter setting reference in the literature [12].

BMP-2 infected MSCs combined with nHA/PA66 culture and bone orientation induction

Culture

We designed four groups: MSCs (cell blank control), MSCs + BMP-2 (cell infection BMP-2), MSCs

+ nHA/PA66 (cell composite scaffold), MSCs + BMP-2 + nHA/PA66 (infected cell composite scaffold). We cultured bone marrow MSCs and nHA/PA66 of the 3rd generation rats in a 24-well plate. We cut the material into 0.3 cm × 0.3 cm × 0.3 cm pieces and disinfected at high temperature and pressure for use. Before composite culture, the handlers cut nHA/PA66 in an osteogenic medium for 24 h. They digested the cells with 0.25 % trypsin and centrifuged, then re-suspended the cells and adjusted the cell concentration to 1.0×10^8 cells/l. 1 ml cell suspension was uniformly inoculated on the pretreated nHA/PA66 scaffold material using a micropipette to form a cell-material complex. After inoculation, we incubated the cells in the incubator at 37 °C and 5 % CO₂ saturation humidity for 4 h and slowly added the osteogenic induction medium. Then, we slightly the liquid surface above the surface of the nHA/PA66 scaffold material to facilitate the full growth of the cells in the nHA/A66 scaffold (composite) and continued to culture in the incubator at 37 °C and 5 % CO₂. Change liquid every 2 days. We determined cell viability by CCK8 at 24 h, 48 h, 72 h, and 96 h after culture.

Detection of MSC adhesion to nHA/PA66

At the 3rd week of osteogenic induction, the 4 groups were fixed with 3 % glutaraldehyde for 24 h, washed 3 times with PBS, and fixed with 1 % osmic acid for 2 h, then eluted with ethanol step by step, replaced with isoamyl gradient acetate, CO₂ critical point drying, gilded and scanning electron microscope observed the adhesion between stem cells and scaffolds. We selected ten non-overlapping 100× visual fields to observe the total cell scaffolds. Select each test 3 times and average the final value.

Detection of alkaline phosphatase (ALP) activity by enzymolysis assay

Extract the 3rd generation rat bone marrow MSCs. Digest the cells with pancreatic enzyme on the 7th day of bone formation induction. Remove the supernatant, add 300 μ l PBS for suspension after centrifugation at 1000 RPM/min for 10 min, and break the cell suspension by ultrasound. To determine alkaline phosphatase activity, refer to the kit instructions. The cells were scraped and treated at 150 μ l 0.05 % Triton X-100 at room temperature for 10 min, followed by ultrasonic treatment, centrifuged at 12000 RPM/min for 10 min. Then, we took the supernatant. The absorbance value (OD) was determined at

405 nm using an enzyme-labeler according to the instructions of the ALP kit.

Establishment of bone nonunion model and implantation of MSCs-(BMP-2)-nHA/PA66 material

We established the rat model of femoral bone nonunion in the article reported [13]. We randomly divided twenty-five SD rats into 4 groups: Blank control group (Model group, nothing implanted), MSCs (uninfected cell), MSCs + BMP-2 (cell infection BMP-2), MSCs + nHA/PA66 (cell composite scaffold), and MSCs + BMP-2 + nHA/PA66 (infected cell composite scaffold), representing whether infected BMP-2 or composite nHA/PA66 stents. Perform all surgical procedures under sterile conditions. Anaesthetize the rats by intraperitoneal injection of 10% chloral hydrate (3 ml/kg). After the anaesthesia took effect, we placed the rats on the operating table in a lateral flexion position. Make a 2 cm incision on the lateral part of the femur. We separated the skin layer and subcutaneous tissue by layer and exposed the femur from the muscle space of the quadriceps and biceps femur. We bluntly separated the outer membrane of the fractured femur after osteotomy with a line saw. Drill the middle part of nHA/PA66 in the simple scaffold and the cell composite scaffold and strung on the Kirkner needle group. Drill the 0.5 mm Kirkner needle into the pulp cavity from the distal end of the fracture with a hand drill. Then perforated through the knee and retrograde through the distal fracture to the hip. We directly fixed the blank control group with Kirschner's needle. Observe fractures to be in good alignment, without rotation or separation and displacement, give local antibiotic lavage and suture the wound after rinsing with normal saline. After waking, we fed rats in the cage and intramuscularly injected them with penicillin 4×10^4 U for three days.

Detection of inflammatory factors in rats with femoral bone nonunion

We anaesthetized the rats, took abdominal aorta blood, injected them into an anticoagulant tube containing EDTA-Na₂ and aprotinin, and centrifuged plasma at 3000 RPM for 10 min. Detect plasma C-reactive protein (CRP), interleukin-6 (IL-6), and tumor necrosis factor- α (TNF- α) by ELISA kit. Measure the Erythrocyte Sedimentation Rate (ESR) by a capillary dynamic photometer.

Statistical analysis

We applied the SPSS 23.0 software package and an independent sample *t*-test for experimental data. Analyze the expression difference of inflammation-related genes between bone non-union samples and healthy samples with the "limma" package in R language. The definition criterion of significant difference was $P < 0.05$.

Results

Up-regulated inflammation-related genes in bone nonunion patients

There were 41 significantly different genes between the patients with acute bone injury nonunion and the healthy volunteers (Fig. 1A), and 26 genes associated with inflammation intermingled with each other (Fig. 1B). The expression of these genes was up-regulated in the patients with acute bone injury nonunion (Table 1). These 26 differential genes were mainly enriched in innate immune response, extracellular region, calcium ion binding, Pantothenate and CoA biosynthesis pathways (Fig. 1C).

Morphological observation, BMP-2 transfection, and expression of MSC cells after isolation

Flow cytometry showed that CD90 and CD29 were expressed in more than 95% of MSCs. In addition, these cells lack the expression of CD45 and CD34 (Fig. 2A).

MSCs were spherical and mostly suspended in a culture medium at the beginning of injection. At 24 h, the cells were mostly round and adherent cells appeared. At 48 h, most cells were adherent and extended, and the volume was slightly larger than the primary cells. At 72 h, fibroid cells appeared. At day 7, most of the cells were fusiform, and the cells still maintained good growth and proliferation ability (Fig. 2B).

After MSCs transfected with BMP-2, we performed fluorescence staining. Fluorescence microscopy showed that green fluorescence was distributed in the whole cell, showing cytoplasmic distribution, indicating that BMP-2 could express in MSCs (Fig. 2C).

The expression level of BMP-2 in the Lent-BMP-2 group [(121.42±29.16) pg/ml] was higher than that in the empty lentivirus vector group [(76.33±20.56) pg/ml] ($t=3.996, P<0.001$) and uninfected groups [(68.55±3.22) pg/ml] ($t=5.699, P<0.001$) (Fig. 2D).

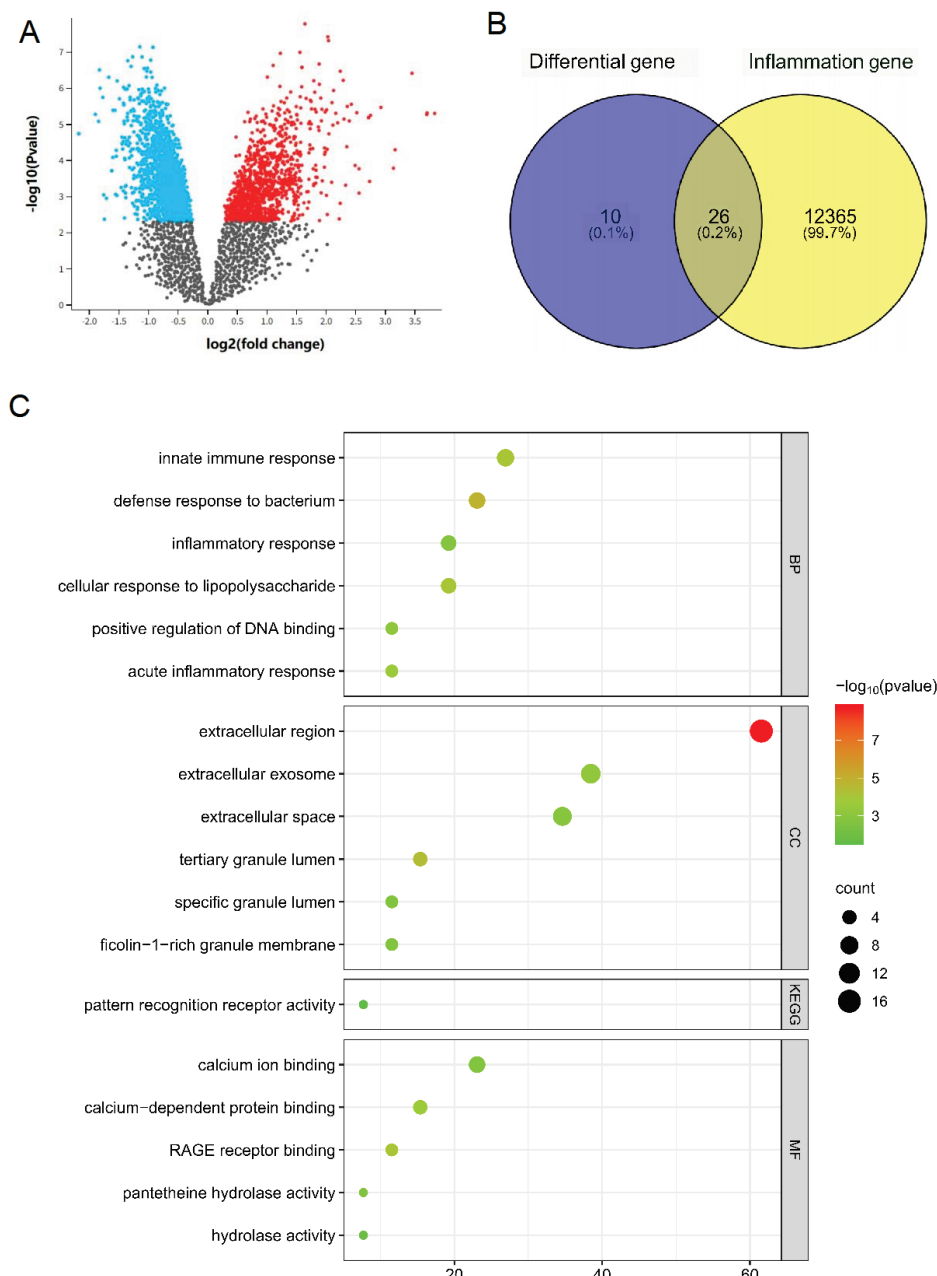


Fig. 1. Differential genes and enrichment analysis related to inflammation.

ALP activity and OD value of MSCs transfected with BMP-2

ALP is one of the phenotypic markers of osteoblast, which can directly reflect the activity or function of osteoblast. After transfection of MSCs with BMP-2, ALP staining was positive, and grain-brown to dark black granular or flaky-like precipitation appeared in the cytoplasm (Fig. 3A).

After BMP-2 and nHA/PA66 induction culture for 7 days, the OD value of ALP in bone tissues of MSCs + BMP-2 + nHA/PA66 group was higher than that of the other 3 groups (all $P<0.05$) (Fig. 3B).

Cell viability of MSCs transfected with BMP-2 and nHA/PA66 and their adhesion to nHA/PA66

The cell viability of MSCs transfected with BMP-2 and nHA/PA66 was determined by the CCK8 method, which showed that the cell viability of MSCs + BMP-2 + nHA/PA66 group was gradually increased. At 96 h, the cell viability of MSCs + BMP-2 and MSCs + nHA/PA66 groups was lower than that of MSCs + BMP-2 and MSCS + NHA /PA66 groups was higher than that of MSCS + BMP-2 and MSCS + NHA/PA66 groups ($P<0.05$) (Fig. 4A).

Table 1. 26 inflammatory genes with significant differences ($\bar{x} \pm s$).

ID	Log FC	adj. P. Val	B	t
<i>LIPN</i>	3.8328400	0.001113	4.470491	7.3197982
<i>ANXA3</i>	3.7053250	0.001113	4.500211	7.3407445
<i>S100A12</i>	3.6996387	0.001128	4.406022	7.2745150
<i>TNFAIP6</i>	3.4496425	0.000533	6.871323	9.1790051
<i>MMP9</i>	3.1653187	0.003158	2.230015	5.8557468
<i>ARG1</i>	3.1369412	0.005939	1.077884	5.1749142
<i>S100A8</i>	2.9245050	0.001060	4.834913	7.5798288
<i>VNN1</i>	2.7339737	0.009737	0.251201	4.7085642
<i>HP</i>	2.5557988	0.006071	1.041476	5.1540254
<i>CLEC4D</i>	2.5556563	0.014923	-0.477817	4.3090663
<i>RNASE2</i>	2.5174900	0.001113	4.513325	7.3500020
<i>LILRA5</i>	2.4257937	0.000975	5.020536	7.7150232
<i>HORMAD1</i>	2.3569475	0.001030	4.894074	7.6227117
<i>HMGB2</i>	2.3488337	0.002866	2.415460	5.9693042
<i>S100P</i>	2.3023450	0.001251	4.126057	7.0802759
<i>QPCT</i>	2.2876550	0.000669	6.457707	8.8318297
<i>MGAM</i>	2.2384125	0.000508	6.995129	9.2854191
<i>ANKRD22</i>	2.2216087	0.044677	-2.083077	3.4521718
<i>TLR5</i>	2.1262587	0.000770	5.855161	8.3476233
<i>SLC22A4</i>	2.0992888	0.000959	5.125361	7.7922190
<i>BCL2A1</i>	2.0926550	0.010057	0.198374	4.6792834
<i>GCA</i>	2.0455163	0.001845	3.216838	6.4746427
<i>VNN2</i>	2.0397325	0.000404	8.752064	10.9376104
<i>BMX</i>	2.0198562	0.037041	-1.810946	3.5964233
<i>TXN</i>	2.0084937	0.001098	4.687667	7.4739184
<i>FCAR</i>	2.0048762	0.016316	-0.622208	4.2309786

In the 3rd week after the combination of rat bone marrow MSCs transfected with BMP-2 and nHA/PA66, the cells spread all over the surface of nHA/PA66 and adhered to each other, and the cells also grew into the pores of the material (Fig. 4B).

Levels of inflammatory cytokines after transfection of MSCs with BMP-2 and nHA/PA66

After implantation of different types of MSCs in nonunion rat models, the levels of inflammatory factors were decreased ($P < 0.05$). The levels of CRP, IL-6, TNF- α , and ESR in the MSCs + BMP-2 + nHA/PA66 group were lower than those in the MSCs and MSCs + nHA/PA66 group but higher than those in MSCs + BMP-2 group (Fig. 5).

Discussion

Inflammation is related to the formation of bone nonunion. We analyzed the gene expression profile of patients with bone nonunion selected from the GEO database, finding that the expression of genes related to inflammation (total of 26 genes) was up-regulated in patients with bone nonunion, consistent with previous studies. These genes, including *LIPN*, *ANXA3*, *S100A12*, and *TNFAIP6*, are the key factors in regulating inflammatory responses. These 26 differential genes were mainly enriched in innate immune response, extracellular region, calcium ion binding, pantothenate and CoA biosynthesis pathways. The innate immune response includes humoral immune abnormality, cellular immune abnormality, complement system abnormality, phagocyte abnormality, etc. Inflammation is a physiological response triggered by the innate immune system. The

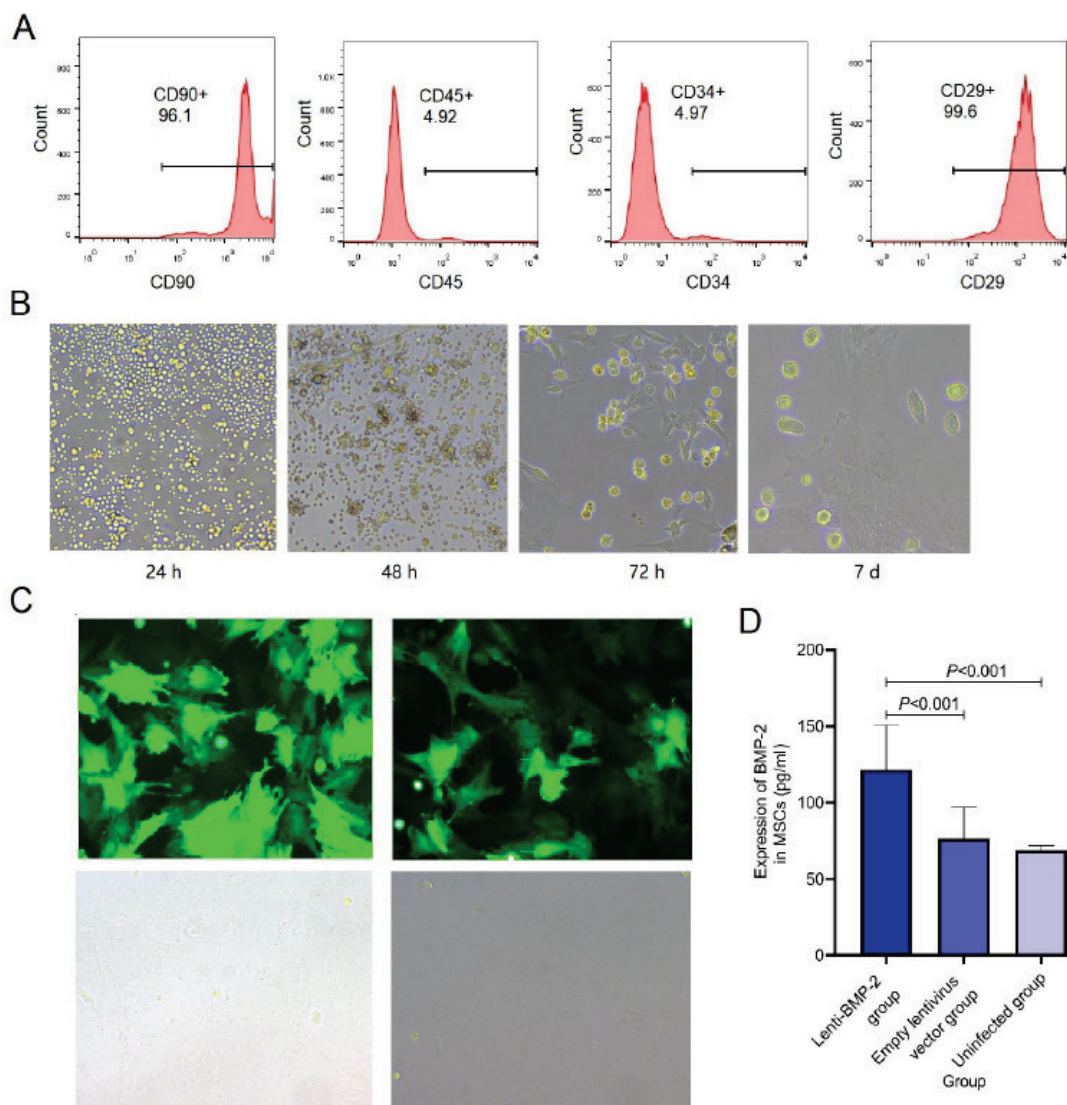


Fig. 2. Morphological observation, BMP-2 transfection, and expression of MSCs cells after isolation.

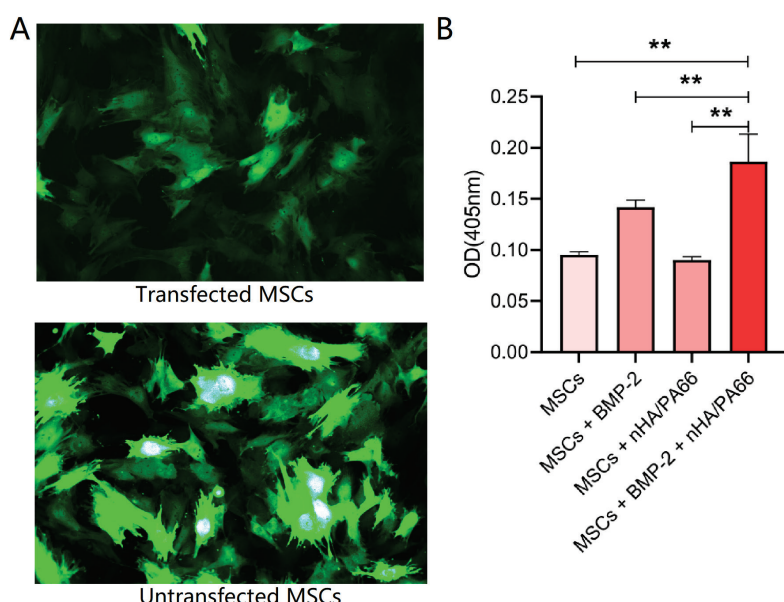


Fig. 3. ALP activity and OD value of MSCs transfected with BMP-2. **(A)** ALP activity. **(B)** OD value of the ALP. * $P<0.05$.

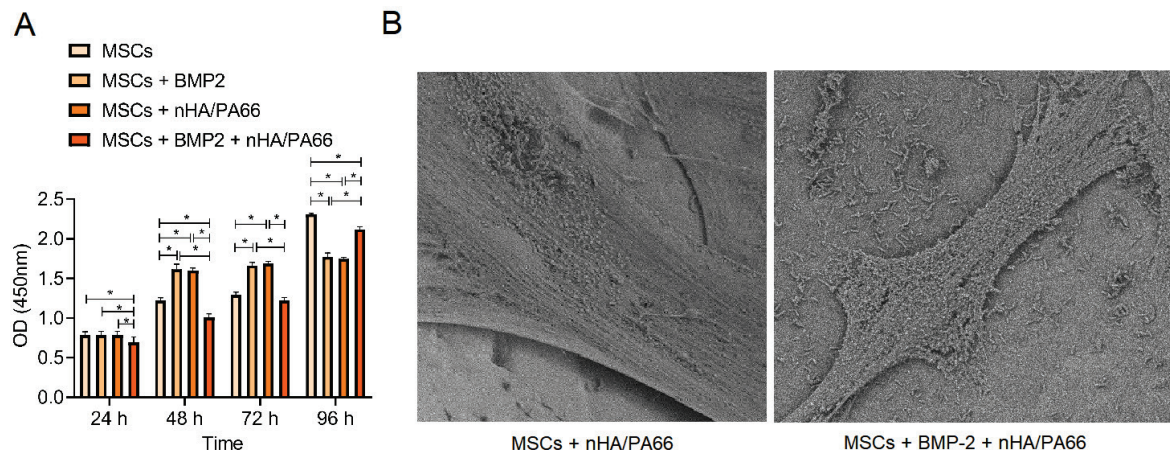


Fig. 4. Cell viability of MSCs transfected with BMP-2 and nHA/PA66 and their adhesion to nHA/PA66. **(A)** MSCs activity level. **(B)** Adhesion on nHA/PA66. * $P < 0.05$.

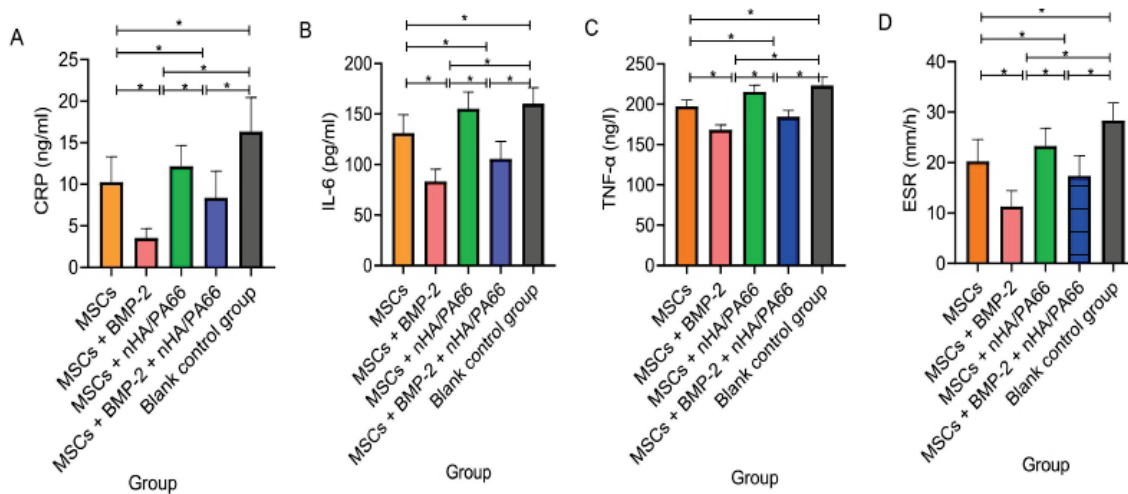


Fig. 5. Levels of inflammatory cytokines after transfection of MSCs with BMP-2 and nHA/PA66. **(A)** CRP. **(B)** IL-6. **(C)** TNF- α . **(D)** ESR. * $P < 0.05$.

human body encounters the invasion of foreign harmful microorganisms that activate the immune system and cause inflammation [14]. The Extracellular matrix (ECM) in the extracellular region is a three-dimensional structure secreted by animal cells and wrapped outside the cell. Its unique network fiber structure is the “landing zone” of inflammatory cells. After crossing the endothelial barrier, white blood cells are “netted” by ECM, and their adhesion, retention, migration and activation are affected, thus shortening the duration of the inflammatory response [15]. The change in intracellular calcium concentration is closely related to the occurrence of inflammatory response. When a stimulus enters the cell, the concentration of calcium ions is briefly increased (calcium imbalance), which increases the secretion of inflammatory mediators and stimulates cell activation. Pantothenate can enhance the activity of immune cells

and participate in the regulation of inflammation [16]. The inflammatory response is accompanied by an imbalance in the oxidation-antioxidant levels within the cell (oxidative stress). Coenzyme A (CoA) can inhibit the production of free radicals and reduce the damage to cells caused by oxidative stress [17].

Based on this, we infected rat MSCs with BMP-2 and transplanted the tissue-engineered bone constructed by combining the cells with nHA/PA66 into the femoral fracture of SD rats in the bone non-union model. The expression level of BMP-2 in the Lenti-BMP-2 group was the highest, indicating that the BMP-2 gene had successfully infected MSCs. After that, we combined MSCs infected with BMP-2 and nHA/PA66 materials to bone construct tissue-engineered, and obtained MSCs + BMP-2 + nHA/PA66 cells with gradually increased cell vitality, indicating good cell activity and suitable for

further research. MSCs + BMP-2 + nHA/PA66 group had positive ALP staining, and the OD value of ALP was the highest, indicating that it formed mineralized nodules after BMP-2 infected MSCs combined with nHA/PA66 material. The ALP activity was strong. ALP is considered to be a marker of osteogenic differentiation and functional status of BMSCs [18]. ALP is a functional enzyme of osteoblasts and plays a key role in calcium salt deposition. ALP can hydrolyze organophosphate, increase the concentration of local phosphate, block calcification inhibitors, and initiate calcification, so the increase of ALP activity marks the differentiation of stem cells into osteoblasts. It can be seen that BMP-2 and nHA/PA66 jointly promote the differentiation of MSCs into osteoblasts, promote the calcium deposition of cells, and enhance the activity of ALP. In addition, the number of adhesion cells in the MSCs + BMP-2 + nHA/PA66 group was higher than that in the other 3 groups, suggesting that BMP-2 and nHA/PA66 not only increased the formation of calcium nodules in BMSCs but also enhanced the adhesion ability of BMSCs.

The growth and proliferation activity of bone marrow BMSC cells and their adhesion to nHA/PA66 were good, indicating that nHA/PA66 scaffold material was suitable for adhesion, proliferation and osteogenic differentiation of bone marrow BMSCs. Therefore, we believe that after transfection of MSCs with BMP-2 and combination with nHA/PA66, BMSCs have good proliferation, growth and osteogenesis ability. Firstly, intramembranous ossification is a new reticular bone formed by osteoblasts through proliferation, differentiation and calcification, which is an important process of bone healing [19]. The osteoblasts are differentiated from bone marrow MSCs. The number of bone marrow MSCs in the bone non-union area was significantly reduced [20]. Bone marrow MSCs are the key to bone healing, and the application of bone marrow MSCs as seed cells in bone tissue engineering to treat bone nonunion has a unique advantage. Secondly, BMP-2 can induce bone marrow MSCs to differentiate into osteoblasts, and promote cell proliferation and collagen synthesis [21]. Many studies have reported that BMP-2 can effectively treat bone defects, bone nonunion and osteoporosis [22,23]. When the body responds to infection, the BMP pathway is activated to effectively regulate cell differentiation and proliferation and participate in cellular immune response [24]. BMP-2 is actively expressed in inflammatory tissues but hardly expressed in normal tissues, suggesting that BMP-2 may

be an important osteogenic factor in bone inflammation [25]. In addition, the composition and structure of nHA/PA66 can fully simulate bone because the inorganic component is nano-hydroxyapatite, and the organic component PA66 is similar to the molecular structure of collagen. Bone regeneration in non-connected areas requires bone formation, the formation of blood vessels and a suitable mechanical environment [26]. The porosity of nHA/PA66 can reach 70 %, and the pore size is between 200-500 μm . The interconnected micropores can create a good three-dimensional space for blood vessel introduction, thus facilitating the formation of blood vessels in the non-connected areas [27]. Li *et al.* [28] found that cross-linking nHA/PA66 with QK ((a VEGF mimetic peptide)) and BMP-2-derived peptides could prevent femoral nonunion in rats. Liu *et al.* [29] showed that MSCs combined application and nHA/PA66 could promote angiogenesis and bone regeneration of large bone defects. The above studies fully demonstrated that the adhesion and proliferation of bone marrow MSCs on nHA/PA66 enabled tissue-engineered bone to have biological activity, successfully enhanced fracture healing and prevented the occurrence of bone nonunion.

We implanted the cell material complex into the femoral fracture of SD rats with the bone-free model and found that the levels of CRP, IL-6, TNF- α and ESR in MSCs + BMP-2 + nHA/PA66 group were lower than those in MSCs and MSCs + nHA/PA66 group, but higher than those in MSCs + BMP-2 group. nHA/PA66 implantation only prevents bone nonunion, but it produces an immune response to transplantation, resulting in increased levels of inflammatory factors. However, complex BMP-2 can reduce inflammation, indicating that BMP-2 can reduce inflammation to a certain extent. Therefore, we speculated that after BMP-2 infected MSCs and combined with nHA/PA66, the osteogenic ability of the fracture end was increased, and BMP-2 might play a role in alleviating the inflammatory response after fracture, and further promoting the oriented differentiation of MSCs into osteoblasts. Inflammatory factors such as CRP, TNF- α and IL-6 are the driving factors of inflammation. When inflammation occurs, ESR increases. Previous studies have suggested that fracture nonunion is due to the overproduction of cytotoxic and pro-apoptotic factors and the dysfunction of morphogenetic protein expression in chronic inflammation [30]. Biological changes associated with bone nonunion, such as systemic immune disorders, can lead to an unfavorable healing environment [31].

Downregulation of bone nonunion inflammation may be another pathway by which MSCs infected with BMP-2 and nHA/PA66 materials promote bone formation. However, more solid research data is needed to support this idea.

Conclusions

The expression level of inflammation-related genes increased in patients with bone nonunion, and the infection of MSCs by BMP-2 promoted the directed

differentiation of MSCs into osteoblasts in rat bone marrow and ALP activity, and reduced inflammation in rats with bone nonunion.

Conflict of Interest

There is no conflict of interest.

Acknowledgements

Qinghai Province Natural Science Foundation Youth Project Grant No. 2022-ZJ-968Q.

References

1. Deng AD, Innocenti M, Arora R, Gabl M, Tang JB. Vascularized Small-Bone Transfers for Fracture Nonunion and Bony Defects. *Clin Plast Surg* 2020;47:501-520. <https://doi.org/10.1016/j.cps.2020.06.005>
2. Lv S, Wang G, Dai L, Wang T, Wang F. Cellular and Molecular Connections Between Bone Fracture Healing and Exosomes. *Physiol Res* 2023;72:565-574. <https://doi.org/10.33549/physiolres.935143>
3. Xu J, Li Z, Tower RJ, Negri S, Wang Y, Meyers CA, Sono T, ET AL. NGF-p75 signaling coordinates skeletal cell migration during bone repair. *Sci Adv* 2022;8:eabl5716. <https://doi.org/10.1126/sciadv.abl5716>
4. Sekiguchi H, Inoue G, Shoji S, Tazawa R, Kuroda A, Miyagi M, Takaso M, Uchida K. Expression of nerve growth factor in the callus during fracture healing in a fracture model in aged mice. *Biomed Mater Eng* 2022;33:131-137. <https://doi.org/10.3233/BME-211284>
5. Goodnough LH, Goodman SB. Relationship of Aging, Inflammation, and Skeletal Stem Cells and Their Effects on Fracture Repair. *Curr Osteoporos Rep* 2022;20:320-325. <https://doi.org/10.1007/s11914-022-00742-x>
6. Liu X, Min HS, Chai Y, Yu X, Wen G. Masquelet technique with radical debridement and alternative fixation in treatment of infected bone nonunion. *Front Surg* 2022;9:1000340. <https://doi.org/10.3389/fsurg.2022.1000340>
7. Prakash N, Kim J, Jeon J, Kim S, Arai Y, Bello AB, Park H, Lee SH. Progress and emerging techniques for biomaterial-based derivation of mesenchymal stem cells (MSCs) from pluripotent stem cells (PSCs). *Biomater Res* 2023;27:31. <https://doi.org/10.1186/s40824-023-00371-0>
8. Chae DS, Han S, Lee MK, Kim SW. BMP-2 Genome-Edited Human MSCs Protect against Cartilage Degeneration via Suppression of IL-34 in Collagen-Induced Arthritis. *Int J Mol Sci* 2023;24:8223. <https://doi.org/10.3390/ijms24098223>
9. Li YL, Zhao WK, Zhang J, Xiang C, Chen Q, Yan C, Jiang K. In vitro and in vivo evaluations of nano-hydroxyapatite/polyamide 66/yttria-stabilized zirconia as a novel bioactive material for bone screws: Biocompatibility and bioactivity. *J Biomater Appl* 2020;35:108-122. <https://doi.org/10.1177/0885328220916618>
10. Zhao W, Li Y, Zhou A, Chen X, Li K, Chen S, Qiao B, Jiang D. Controlled release of basic fibroblast growth factor from a peptide biomaterial for bone regeneration. *R Soc Open Sci* 2020;7:191830. <https://doi.org/10.1098/rsos.191830>
11. Shabir U, Bhat IA, Pir BA, Bharti MK, Pandey S, Gutulla SK, Sarkar M, ET AL. Smad4 and γ -secretase knock-down effect on osteogenic differentiation mediated via Runx2 in canine mesenchymal stem cells. *Res Vet Sci* 2022;145:116-124. <https://doi.org/10.1016/j.rvsc.2022.02.004>
12. Ye W, Huang Y, Zhu G, Yan A, Liu Y, Xiao H, Mei H. miR-30a inhibits the osteogenic differentiation of the tibia-derived MSCs in congenital pseudarthrosis via targeting HOXD8. *Regen Ther* 2022;21:477-485. <https://doi.org/10.1016/j.reth.2022.09.005>
13. Elias D, Ditzel HJ. Fyn is an important molecule in cancer pathogenesis and drug resistance. *Pharmacol Res* 2015;100:250-254. <https://doi.org/10.1016/j.phrs.2015.08.010>
14. Ma H, Liu M, Fu R, Feng J, Ren H, Cao J, Shi M. Phase separation in innate immune response and inflammation-related diseases. *Front Immunol* 2023;14:1086192. <https://doi.org/10.3389/fimmu.2023.1086192>

15. Marozzi M, Parnigoni A, Negri A, Viola M, Vigetti D, Passi A, Karousou E, Rizzi F. Inflammation, Extracellular Matrix Remodeling, and Proteostasis in Tumor Microenvironment. *Int J Mol Sci* 2021;22:8102. <https://doi.org/10.3390/ijms22158102>
16. Zhang Y, Li G, Zhao Y, Dai X, Hu M, Cao H, Huang K, Yang F. Inhibition of calcium imbalance protects hepatocytes from vanadium exposure-induced inflammation by mediating mitochondrial-associated endoplasmic reticulum membranes in ducks. *Poul Sci* 2023;102:103013. <https://doi.org/10.1016/j.psj.2023.103013>
17. Yeudall S, Upchurch CM, Seegren PV, Pavelec CM, Greulich J, Lemke MC, Harris TE, ET AL. Macrophage acetyl-CoA carboxylase regulates acute inflammation through control of glucose and lipid metabolism. *Sci Adv* 2022;8:eabq1984. <https://doi.org/10.1126/sciadv.abq1984>
18. Nirwan N, Vohora D. Linagliptin in Combination With Metformin Ameliorates Diabetic Osteoporosis Through Modulating BMP-2 and Sclerostin in the High-Fat Diet Fed C57BL/6 Mice. *Front Endocrinol (Lausanne)* 2022;13:944323. <https://doi.org/10.3389/fendo.2022.944323>
19. Ghimire S, Miramini S, Edwards G, Rotne R, Xu J, Ebeling P, Zhang L. The investigation of bone fracture healing under intramembranous and endochondral ossification. *Bone Rep* 2020;14:100740. <https://doi.org/10.1016/j.bonr.2020.100740>
20. Mathieu M, Rigutto S, Ingels A, Spruyt D, Stricwant N, Kharroubi I, Albarani V, Jayankura M, Rasschaert J, Bastianelli E, Gangji V. Decreased pool of mesenchymal stem cells is associated with altered chemokines serum levels in atrophic nonunion fractures. *Bone* 2013;53:391-398. <https://doi.org/10.1016/j.bone.2013.01.005>
21. Gao S, Chen B, Zhu Z, Du C, Zou J, Yang Y, Huang W, Liao J. PI3K-Akt signaling regulates BMP2-induced osteogenic differentiation of mesenchymal stem cells (MSCs): A transcriptomic landscape analysis. *Stem Cell Res* 2023;66:103010. <https://doi.org/10.1016/j.scr.2022.103010>
22. Kendal JK, Singla A, Affan A, Hildebrand K, Al-Ani A, Ungrin M, Mahoney DJ, ET AL. Is Use of BMP-2 Associated with Tumor Growth and Osteoblastic Differentiation in Murine Models of Osteosarcoma? *Clin Orthop Relat Res* 2020;478:2921-2933. <https://doi.org/10.1097/CORR.0000000000001422>
23. Yi M, Nie Y, Zhang C, Shen B. Application of Mesoporous Silica Nanoparticle-Chitosan-Loaded BMP-2 in the Repair of Bone Defect in Chronic Osteomyelitis. *J Immunol Res* 2022;2022:4450196. <https://doi.org/10.1155/2022/4450196>
24. Nie X, Sun X, Wang C, Yang J. Effect of magnesium ions/Type I collagen promote the biological behavior of osteoblasts and its mechanism. *Regen Biomater* 2020;7:53-61. <https://doi.org/10.1093/rb/rbz033>
25. Shen J, James AW, Zara JN, Asatrian G, Khadarian K, Zhang JB, Ho S, ET AL. BMP2-induced inflammation can be suppressed by the osteoinductive growth factor NELL-1. *Tissue Eng Part A* 2013;19:2390-2401. <https://doi.org/10.1089/ten.tea.2012.0519>
26. Khan S, Peracha A, Abro AA, Sufyan M, Rahim Najjad MK, Aziz S, Khan MM. Clinical studies investigating the role of mesenchymal stem cells in healing of fracture non-unions: a systematic review. *J Pak Med Assoc* 2023;73(Suppl 1):S26-S31. <https://doi.org/10.47391/JPMA.AKUS-05>
27. Zou Q, Li J, Niu L, Zuo Y, Li J, Li Y. Modified n-HA/PA66 scaffolds with chitosan coating for bone tissue engineering: cell stimulation and drug release. *J Biomater Sci Polym Ed* 2017;28:1271-1285. <https://doi.org/10.1080/09205063.2017.1318029>
28. Li A, Li J, Zhang Z, Li Z, Chi H, Song C, Wang X, ET AL. Nanohydroxyapatite/polyamide 66 crosslinked with QK and BMP-2-derived peptide prevented femur nonunion in rats. *J Mater Chem B* 2021;9:2249-2265. <https://doi.org/10.1039/D0TB02554B>
29. Liu W, Huang Y, Liu D, Zeng T, Wang J, Li A, Wang D, Wang X. The Combination of Platelet Rich Plasma Gel, Human Umbilical Mesenchymal Stem Cells and Nanohydroxyapatite/polyamide 66 Promotes Angiogenesis and Bone Regeneration in Large Bone Defect. *Tissue Eng Regen Med* 2022;19:1321-1336. <https://doi.org/10.1007/s13770-022-00471-3>
30. Kostiv RE, Matveeva NY, Kalinichenko SG. Localization of VEGF, TGF- β 1, BMP-2, and Apoptosis Factors in Hypertrophic Nonunion of Human Tubular Bones. *Bull Exp Biol Med* 2022;173:160-168. <https://doi.org/10.1007/s10517-022-05513-3>
31. Vantucci CE, Krishan L, Cheng A, Prather A, Roy K, Guldberg RE. BMP-2 delivery strategy modulates local bone regeneration and systemic immune responses to complex extremity trauma. *Biomater Sci* 2021;9:1668-1682. <https://doi.org/10.1039/D0BM01728K>